INFLUENCE OF BODY SHAPE ON THE SPATIAL BOUNDARY LAYER CHARACTERISTICS ON A PERMEABLE SURFACE

A. I. Borodin and S. V. Peigin

UDC 532.526

Results are presented of computations of the flow of a homogeneous gas in the spatial laminar boundary layer on blunt bodies of different shape with a permeable surface around which are flows at angles of attack and slip.

Investigation of the fundamental flow characteristics in a three-dimensional boundary layer on bodies around which a supersonic gas flows is necessary for the solution of many applied problems. The papers [1-8] are devoted to a study of this problem. Solutions are obtained in [1-4] for the boundary layer equations around bodies with an impermeable surface. The case of a permeable surface was examined in [5-8]; however, the computations were performed here either in the neighborhood of the plane of symmetry [5] or when there are two planes of symmetry in the flow [6-8]. At the same time it is interesting to analyze the influence of body geometry and gas injection from the surface on the heat and mass transfer characteristics for the general case of the flow around a body at angles of attack and slip.

Let us consider the flow of a homogeneous compressible gas in a three-dimensional laminar boundary layer on blunt bodies with a permeable surface around which a hypersonic gas flows. In a curvilinear (ξ, η, ζ) coordinate system in which ζ is measured along the normal to the body, and ξ, η are selected in a certain way on the surface, the equations describing this flow have the following dimensionless form [4]:

$$\frac{\partial}{\partial\xi}\left(\rho u\sqrt{\frac{g}{g_{11}}}\right)+\frac{\partial}{\partial\eta}\left(\rho w\sqrt{\frac{g}{g_{22}}}\right)+\frac{\partial}{\partial\zeta}(\rho v\sqrt{g})=0,$$

$$\rho(Du+A_1u^2+A_2uw+A_3w^2)=A_4+\frac{\partial}{\partial\zeta}\left(\mu\frac{\partial u}{\partial\zeta}\right),$$

$$\rho(Dw+B_1u^2+B_2uw+B_3w^2)=B_4+\frac{\partial}{\partial\zeta}\left(\mu\frac{\partial w}{\partial\zeta}\right),$$

$$\rho DT=\frac{\gamma-1}{\gamma}D^{\circ}P+\frac{\partial}{\partial\zeta}\left(\frac{\mu}{\sigma}\frac{\partial T}{\partial\zeta}\right)+2\mu\left[\left(\frac{\partial u}{\partial\zeta}\right)^2+\left(\frac{\partial w}{\partial\zeta}\right)^2+2\cos\psi\frac{\partial u}{\partial\zeta}\frac{\partial w}{\partial\zeta}\right], \tag{1}$$

$$P=\rho T,\quad \mu=T^{\omega},\quad D\equiv D^{\circ}+v\frac{\partial}{\partial\zeta},$$

$$D^{\circ}\equiv\frac{u}{\sqrt{g_{11}}}\frac{\partial}{\partial\xi}+\frac{w}{\sqrt{g_{22}}}\frac{\partial}{\partial\eta}.$$

Here the quantities A_i, B_i depend in a known manner on the pressure distribution along the surface and on the component $g_{\alpha\beta}$ [4]. The system (1) is solved under the following boundary conditions:

$$\zeta=0:\quad u=w=0,\ (\rho v)_w=G(\xi,\eta),\ T=T_w(\xi,\eta), \tag{2}$$

$$\zeta=\infty:\quad u=u_e(\xi,\eta),\ w=w_e(\xi,\eta),\ T=T_e(\xi,\eta). \tag{3}$$

We select the (ξ, η) coordinate system on the body surface in the following way. Let $\{x^i\}$ be a Cartesian coordinate system in which the equation of the surface of the streamlined body has the form $F(x^1, x^2, x^3) = 0$ and $l(\cos\alpha, \sin\alpha\cdot\sin\beta, \sin\alpha\cdot\cos\beta)$ is the unit vector that agrees with the free stream velocity vector in direction. Furthermore, we go over to another Cartesian coordinate system $\{z^i\}$ by the formula

Scientific-Research Institute of Applied Mathematics and Mechanics at Tomsk State University. Translated from Inzhenerno-Fizicheskii Zhurnal, Vol. 53, No. 3, pp. 365-373, September, 1987. Original article submitted May 29, 1986.

 0022-0841/87/5303-0994$12.50

$$x - x_0 = \Lambda(Az), \tag{4}$$

where Λ is a diagonal matrix defining the compression (tension) transformation, A is a matrix giving the rotation of the coordinate axes in such a manner that the axis z^1 would be directed along the internal normal of the body. We introduce a spherical coordinate system with center on the z^1 axis at the point B:

$$z^1 - z_B^1 = -r\cos(\Delta\xi), \quad z^2 = r\sin(\Delta\xi)\cos\eta, \quad z^3 = r\sin(\Delta\xi)\sin\eta. \tag{5}$$

The variable η varies between 0 and 2π in the coordinate system selected in this manner, and all the geometric characteristics of the surface and the coefficients of the system (1) are periodic (of period 2π) functions in η. Therefore, the desired function in (1) will also be periodic in η. The periodicity condition for any of them is written in the form

$$\psi|_{\eta=0} = \psi|_{\eta=2\pi}, \quad \left.\frac{\partial\psi}{\partial\eta}\right|_{\eta=0} = \left.\frac{\partial\psi}{\partial\eta}\right|_{\eta=2\pi}. \tag{6}$$

To integrate the problem (1)-(3) numerically it is convenient to go over to new dependent and independent variables by means of the formulas

$$\xi^* = \xi, \quad \eta^* = \eta, \quad \zeta^* = k\int_0^\zeta \rho d\zeta,$$
$$u^* = \frac{u}{u_e} = \frac{\partial\varphi_1}{\partial\zeta^*}, \quad w^* = \frac{w}{w_e} = \frac{\partial\varphi_2}{\partial\zeta^*}, \quad \theta = \frac{T}{T_e}, \tag{7}$$

where k is a certain constant defined below. The original system (1) in the variables (7) takes the form (we omit the superscript *)

$$(lu'_\zeta)'_\zeta = Du + \beta_1(u^2 - \theta) + \beta_2(w^2 - \theta) + \beta_3(uw - \theta),$$
$$(lw'_\zeta)'_\zeta = Dw + \beta_4(w^2 - \theta) + \beta_5(uw - \theta) + \beta_6(u^2 - \theta),$$
$$\left(\frac{l}{\sigma}\theta'_\zeta\right)'_\zeta = D\theta - \alpha_5 l[(u_e u'_\zeta)^2 + (w_e w'_\zeta)^2 + 2\cos\psi u_e w_e u'_\zeta w'_\zeta], \tag{8}$$
$$D \equiv \alpha_1\left(u\frac{\partial}{\partial\xi} - \varphi'_{1\xi}\frac{\partial}{\partial\zeta}\right) + \alpha_2\left(w\frac{\partial}{\partial\eta} - \varphi'_{2\eta}\frac{\partial}{\partial\zeta}\right) - (\alpha_3\varphi_1 + \alpha_4\varphi_2)\frac{\partial}{\partial\zeta}.$$

The coefficients of the system (8) are defined as follows:

$$\alpha_1 = \frac{u_e}{c\sqrt{g_{11}}}, \quad \alpha_2 = \frac{w_e}{c\sqrt{g_{22}}}, \quad \alpha_3 = (c\sqrt{g})^{-1}\frac{\partial}{\partial\xi}\left(u_e\sqrt{\frac{g}{g_{11}}}\right),$$
$$\alpha_4 = (c\sqrt{g})^{-1}\frac{\partial}{\partial\eta}\left(w_e\sqrt{\frac{g}{g_{22}}}\right), \quad \alpha_5 = \frac{2}{T_e},$$
$$l = \frac{\mu\rho}{\mu_e\rho_e} = \theta^{\omega-1}, \quad \beta_1 = c^{-1}\left(\frac{u'_{e\xi}}{\sqrt{g_{11}}} + A_1 u_e\right),$$
$$\beta_2 = A_3\frac{w_e^2}{cu_e}, \quad \beta_3 = c^{-1}\left(2A_2 w_e + \frac{w_e u'_{e\eta}}{u_e\sqrt{g_{22}}}\right), \tag{9}$$
$$\beta_4 = c^{-1}\left(B_3 w_e + \frac{w'_{e\eta}}{\sqrt{g_{22}}}\right), \quad \beta_5 = c^{-1}\left(2B_2 u_e + \frac{u_e w'_{e\xi}}{w_e\sqrt{g_{11}}}\right),$$
$$\beta_6 = \frac{B_1 u_e^2}{cw_e}, \quad c = k^2\mu_e\rho_e.$$

In the new variables the boundary conditions (2) and (3) have the form:

for $\zeta \neq 0$

$$u = w = 0, \quad \theta = \theta_w, \quad \left(u_e\sqrt{\frac{g}{g_{11}}}\varphi_1\right)'_\xi + \left(w_e\sqrt{\frac{g}{g_{22}}}\varphi_2\right)'_\eta = -k(\rho v)_w\sqrt{g}, \tag{10}$$

for $\zeta \to \infty$

$$u = w = \theta = 1. \tag{11}$$

Since the coordinate system (ξ, η, ζ) is degenerate at the critical point $\xi = 0$, a nondegenerate curvilinear coordinate system (y^1, y^2, y^3) with origin at the stagnation point, whose axes Oy^1 and Oy^2 lie in the tangent plane to the body at this point and are directed, respectively, along the directions of principal curvature of the body surface while the axis Oy^3 is along the normal to the body, was used to obtain the solution of the spatial boundary layer equations in the neighborhood of the stagnation point. The coefficients of the system (9) at the stagnation point in this coordinate system take on the following values

$$\alpha_1 = \alpha_2 = \beta_2 = \beta_3 = \beta_5 = \beta_6 = 0, \quad \alpha_5 = 2,$$
$$\beta_1 = \alpha_3 = 1, \quad \beta_4 = \alpha_4 = R_2/R_1. \tag{12}$$

After finding the solution u°, w°, θ° of the system of equations (8)-(11) in the $\{y^i\}$ coordinate system, a conversion is made to the coordinate system (ξ, η, ζ) by means of the formulas

$$u(0, \eta, \zeta) = \frac{u^\circ u_e^\circ \delta_1 + w^\circ w_e^\circ \delta_2}{u_e^\circ \delta_1 + w_e^\circ \delta_2},$$
$$w(0, \eta, \zeta) = \frac{u^\circ u_e^\circ \gamma_1 + w^\circ w_e^\circ \gamma_2}{u_e^\circ \gamma_1 + w_e^\circ \gamma_2}, \quad \theta(0, \eta, \zeta) = \theta^\circ, \tag{13}$$

where δ_1, δ_2, γ_1, γ_2 are the coupling coefficients of the unit vectors of the bases of the coordinate systems (y^1, y^2) and (ξ, η) in a plane tangent to the surface at the stagnation point.

The constant k introduced in the change of variables (7) was selected from the condition that the normal coordinates in the systems $\{y^i\}$ and (ξ, η, ζ) agree at the stagnation point.

For the numerical solution of system (8) with the boundary conditions (10) and (11), a difference scheme was used that is implicit in the direction ζ and has the order of approximation $O(\Delta\xi) + O(\Delta\eta)^2 + O(\Delta\zeta)^4$, which is a generalization of the scheme in [9] to the three-dimensional case. The derivatives in the ξ direction were calculated to first-order accuracy by using "backward differences" while the derivatives with respect to the angular coordinate η were approximated by central differences on the basis of the solution obtained in the preceding global iteration in the running neighborhood ξ = const. Then each third-order equation in the variable ζ was reduced to a system of three first-order equations by the introduction of new independent functions, and then linearized in an appropriate manner and approximated by finite differences to $O(\Delta\zeta)^4$ accuracy.

The pressure distribution along the surface was considered known in the computation of the parameters on the outer boundary of the boundary layer and was found by the Newton formula. The quantities u_e, w_e, T_e were determined from the system of equations that could be obtained from (1) by omitting the derivatives with respect to ζ and that was solved numerically by using a finite-difference scheme with accuracy $O(\Delta\xi) + O(\Delta\eta)^2$ of the approximation. The obtained system of transcendental equations was linearized with respect to the corrections to the desired functions and was solved by the cyclic factorization method [10] in the coordinate η.

For $(\rho v)_w \equiv 0$ the last equation in the boundary conditions (10) has the trivial solution $\varphi_1 = \varphi_2 = 0$. In the case of a permeable surface $(\rho v)_w = G(\xi, \eta) > 0$, to determine $\varphi_{1w} = \varphi_{2w} = \varphi_w(\xi, \eta)$ this equation was approximated by finite-differences with the order $O(\Delta\xi) + O(\Delta\eta)^2$ and was also solved numerically by the cyclic factorization method.

A flow was considered at angles of attack and slip around three-axis ellipsoids with different semiaxes for which the equation of the surface in dimensionless coordinates referred to the length of the semiaxis in the Ox^1 direction had the form

$$(x^1 - 1)^2 + \left(\frac{x^2}{b}\right)^2 + \left(\frac{x^3}{a}\right) = 1. \tag{14}$$

In this case the diagonal terms of the matrix Λ in (4) equaled the ellipsoid semiaxes and the equation of its surface in the spherical (ξ, η, r) coordinate system had the form $r = 1$, which shortened the amount of calculational work in determining $g_{\alpha\beta}$. The function $\Delta = \Delta(\eta)$ in (5) was selected in such a manner that the normal to the surface of the streamlined body on the line $\xi = 1$ was perpendicular to the vector 1. The governing parameters of the problem were variated in the following ranges

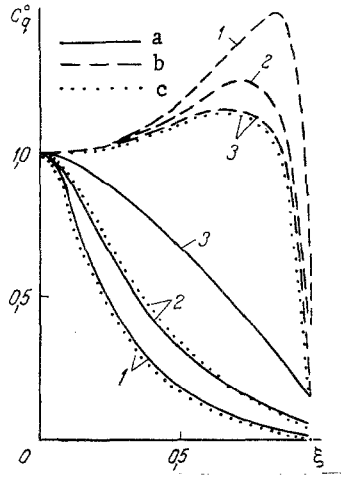

Fig. 1. Dependences of the distribution c_q° on the longitudinal coordinate ξ for different a and b in the sections η = const for $\theta_w = 0.1$, G = 0: 1-3) $\eta = -1.57$, -0.69, 0, respectively; a) $a = 0.3$, b = 0.7; b) $a = 3$, b = 2; c) $a = 0.3$, b = 2.

$$0 < b \leqslant 3, \quad 0 < a \leqslant 3, \quad 0 \leqslant \alpha \leqslant 45^\circ, \quad 0 \leqslant \beta \leqslant 45^\circ, \quad \gamma = 1{,}4,$$
$$\theta_w = 0{,}1, \quad \omega = 0{,}5, \quad 0 \leqslant (\rho v)_w \equiv G = \text{const} \leqslant 2, \quad \sigma = 0{,}71. \tag{15}$$

Computations showed that the proposed numerical method of solving the spatial laminar boundary layer equations on a permeable surface possesses stability and is effective and economical. The mean time for a computation on a BÉSM-6 electronic computer is 70 min for one variant on a 30 × 26 × 15 mesh (in the ξ, η, ζ directions, respectively).

The velocity and temperature profiles across the boundary layer as well as the friction and heat-transfer coefficients on the body surface were determined during the computations, and the expressions for these coefficients in the variables (7) have the form

$$c_\xi = 2k\mu\rho \frac{\partial u}{\partial \zeta}, \quad c_\eta = 2k\mu\rho \frac{\partial w}{\partial \zeta}, \quad c_q = k \frac{\mu\rho}{\sigma} \frac{\partial \theta}{\partial \zeta}. \tag{16}$$

We now turn to a discussion of the numerical computations performed, for which certain results are presented in Figs. 1-3. Analysis of the solutions obtained showed that the distributions of absolute values of the friction and thermal flux coefficients along the body surface depend strongly on its geometry, surface temperature, and gas injection through it. Thus, for example, the difference between the magnitude of c_q computed for $\theta_w = 0.1$ and the value of this same parameter for $\theta_w = 0.5$ is 40-60% depending on the point on the surface and its shape; an increase in G from 0 to 1 (other conditions remaining equal) resulted in a 50-60% diminution in c_q. At the same time computations showed that the heat flux distribution, referred to its value at the stagnation point, is considerably more conservative and depends much more weakly on θ_w and G. In particular, the relative distributions

$$c_\xi^\circ = \frac{c_\xi(\xi, \eta)}{c_\xi(0, \eta)}, \quad c_\eta^\circ = \frac{c_\eta(\xi, \eta)}{c_\eta(0, \eta)}, \quad c_q^\circ = \frac{c_q(\xi, \eta)}{c_q(0, \eta)} \tag{17}$$

are practically independent of the surface temperature θ_w for G = 0 for a cooled surface ($\theta_w \leqslant 0.3$). On the whole, comparisons performed in the above-mentioned range of variation of the body shape, angles of attack and slip showed that for G = 0 the change in c_q° as θ_w varied between 0.05 and 0.3 did not exceed 10%. Gas injection through the surface (for G = const $\leq$ 1) conserves the mentioned regularity, although the range of variation of c_q° increases somewhat (to 15%) as θ_w varies.

At the same time the dependence of the relative heat flux distribution c_q° on the angles of attack and slip as well as on the body shape, determined in this case by the ellipsoid semiaxes a and b, remains sufficiently strong. If $\alpha = \beta = 0$, then there are two planes of symmetry in the flow in which the solutions are independent of each other while the heat flux distribution c_q° has local extremums in these planes. The nature of these extremums here depends on a and b. Figure 1 illustrates this deduction where it is seen that for a =

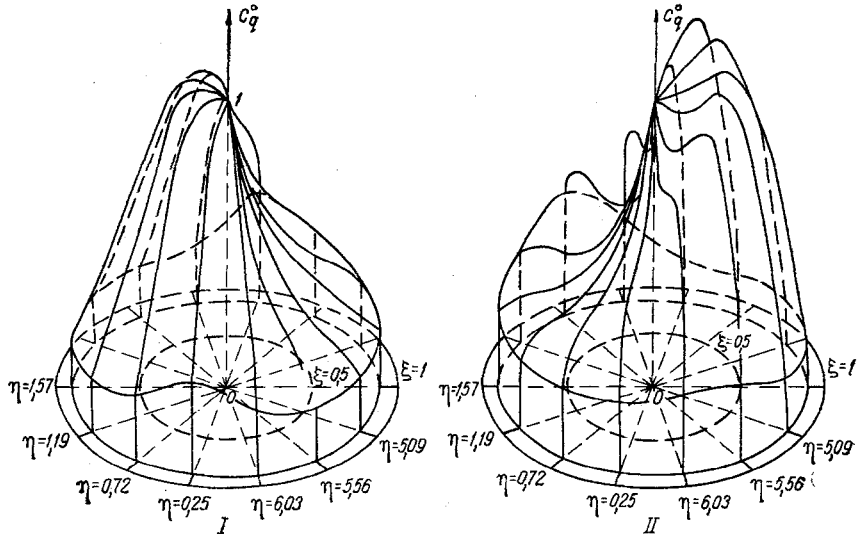

Fig. 2. Distribution of c_q° along an impermeable ellipsoid surface (I — a = 0.3, b = 0.7; II — a = 3, b = 2) for θ_w = 0.25, G = 0, $\alpha = \beta = 45°$.

0.3, b = 0.7 the stagnation point is a local maximum point in the heat flux distribution, a local minimum of c_q° is at the stagnation point for a = 3, b = 2, and the stagnation point turns out to be a saddle point in the c_q° distribution for a = 0.3, b = 2 (the heat flux in the plane x^1Ox^3 drops during standoff from the stagnation point and grows in the x^1Ox^2 plane). Such a dependence of the heat flux distribution in the neighborhood of the stagnation point has a sufficiently explicit physical meaning. Indeed, it is known that the heat flux drops as the gas temperature diminishes on the outer boundary layer boundary and grows as the energy liberation increases within the boundary layer because of viscous dissipation, which is, in turn, inversely proportional to the radius of longitudinal curvature of the body contour in this plane. In this connection, for a < 1, b < 1 when these radii in the planes of symmetry grow with distance from the stagnation point, the maximum heat flux is localized in them. If a and b are sufficiently large (for a, b ≥ 1.3), then the radii of curvature drop monotonically as the distance from the stagnation point increases, and magnification of the viscous dissipation starts to predominate over the reasons causing diminution of the heat flux, whereupon the stagnation point becomes a local minimum point in the c_q° direction.

For nonzero angles of attack and β = 0 only one plane of symmetry remains in the flow and the pattern of the c_q° distribution is still more complicated. If a and b are such that a maximum heat flux is realized for a zero angle of attack at the stagnation point, then for angle-of-attack flow around this same body the maximum remains in the plane of flow symmetry, but is shifted from stagnation point towards diminution of the longitudinal radius of curvature of the body contour in its plane of symmetry. As the angle of attack increases, the value of this maximum in c_q° grows and it is itself moved further from the stagnation point. The absolute value of the heat flux as the angle of attack grows will here drop at both the stagnation point and at the local maximum point for c_q°. If a and b lie in the range when the stagnation point is a local minimum point for α = 0, and there are local maximums on the body lateral surface in its planes of symmetry, then an increase in the angle of attack that keeps all the local extremums in the plane of flow symmetry shifts their location. In particular, the local minimum is shifted from the stagnation point towards an increase in the longitudinal curvature of the body contour; one of the local c_q° maximums that is diminishing in its magnitude approaches the stagnation point while the other recedes from it and vanishes for a sufficiently high angle of attack. The absolute value of the heat flux at both the stagnation point and the local maximum point here grows as the angle of attack grows.

If the flow around the body occurs at nonzero angles of attack and slip, then a further complication is observed in the flow structure in the boundary layer and the heat flux distribution pattern along the surface: there are no planes of symmetry in the flow and the c_q° distributions are substantially spatial in nature (see Fig. 2). The computations showed that in this case the c_q° distributions depend on the circumferential coordinate η in a nonmonotonic manner and have a characteristic maximum whose location depends mainly on the body shape. For a < 1, b < 1 (flow around a prolate ellipsoid) the maximum is on the leeward side of the body,

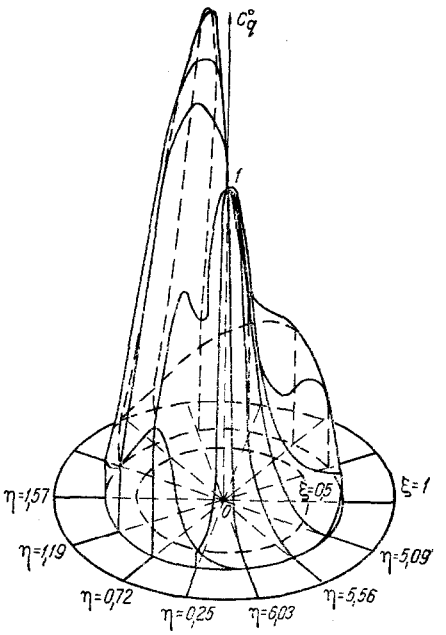

Fig. 3. Distribution of c_q° on an ellipsoid (a = 0.3, b = 0.7) for θ_w = 0.25, G = 2, $\alpha = \beta = 45°$.

and for sufficiently large values of a and b is shifted toward the windward side of the surface. The relative friction coefficient c_ξ° behaves in an analogous manner; moreover, this effect is much stronger for it. On the whole, analysis of the obtained numerical solutions permits making the deduction that the locations of the mentioned maximums in the c_q° and c_ξ° distributions are close to each other and are in the neighborhood of the point with maximal mean surface curvature.

There remains the question of the influence of injection on the fundamental flow characteristics. As computations showed, injection influences the flow structure in the boundary layer sufficiently strongly. As it grows, the velocity and temperature profiles become less inflated, the boundary layer thickness grows, and for G = 1 it increases almost twice as compared with the case of an impermeable surface. An increase in injection results in both magnification of the secondary flow intensity (analogously to the case of flows with two planes of symmetry [6, 7]) and in an increase in the nonmonotonicity in the dependence of the boundary layer thickness on the circumferential coordinate η. As already noted, gas injection results in a significant drop in the absolute values of the friction and heat transfer coefficients on the body surface. At the same time, the influence of injection on the relative quantities c_ξ°, c_q° is much more weakly expressed. In particular, for small and moderate values of the gas mass flow through the surface, the injection does not alter the qualitative pattern of the behavior of c_ξ° and c_q°. As is seen from Fig. 3, the dependences mentioned have the characteristic maximum during injection exactly as on an impermeable surface. The location of this maximum is independent of G in practice and its value grows as the gas mass flow rate through the surface increases.

NOTATION

ξL, ηL, $\zeta L/\sqrt{Re}$, dimensional curvilinear coordinates coupled to the surface of the streamlined body; L, characteristic linear dimension of the problem; $Re = \rho_0 V_0 L/\mu$, Reynolds number; $V_0 = \sqrt{2c_p T_0}$; c_p, coefficient of specific heat; uV_0, wV_0, $vV_0/\sqrt{Re}$, physical components of the velocity vector in the ξ, η, ζ directions, respectively; $\rho_0\rho$, P_0P, T_0T, $\mu_0\mu$, density, pressure, temperature, viscosity coefficient; σ, Prandtl number; ω, exponent in the dependence of the viscosity on the temperature; $g_{\alpha\beta}$, covariant component of the fundamental metric tensor; $g = g_{11}g_{22} - g_{12}^2$; $\cos\psi = g_{12}/\sqrt{g_{11}g_{22}}$; $\Delta = \Delta(\eta)$, normalizing function in the coordinate ξ; R_1, R_2, principal radii of curvature of the body at the stagnation point; α, angle of attack; β, angle of slip; $\gamma = c_p/c_v$, adiabatic index. The subscripts e, w, 0 refer, respectively, to parameters on the outer boundary layer boundary, on the body surface, and on the outer boundary layer boundary at the stagnation point (point of maximum pressure on the body surface).

LITERATURE CITED

1. N. D. Vvedenskaya, Izv. Akad. Nauk SSSR, Mekh. Zhidk. Gaza, No. 5, 36-40 (1966).
2. G. N. Andreev and Yu. D. Shevelev, Izv. Akad. Nauk SSSR, Mekh. Zhidk. Gaza, No. 3, 41-48 (1971).
3. G. A. Tirskii and Yu. D. Shevelev, Prikl. Mat. Mekh., 37, No. 6, 974-983 (1973).
4. Yu. D. Shevelev, Three-Dimensional Problems of Laminar Boundary Layer Theory [in Russian], Moscow (1977).
5. I. G. Brykina, É. A. Gershbein, and S. V. Peigin, Izv. Akad. Nauk SSSR, Mekh. Zhidk. Gaza, No. 5, 37-48 (1980).
6. É. A. Gershbein and S. V. Peigin, Hypersonic Spatial Flows in the Presence of Physicochemical Transformations [in Russian], Moscow (1981), pp. 52-71.
7. I. G. Brykina, É. A. Gershbein, and S. V. Peigin, Izv. Akad. Nauk SSSR, Mekh. Zhidk. Gaza, No. 3, 49-58 (1982).
8. A. I. Borodin and S. V. Peigin, Gas Dynamics [in Russian], Tomsk (1984), pp. 112-119.
9. I. V. Petukhov, Numerical Methods of Solving Differential and Integral Equations and Quadrature Formulas [in Russian], Moscow (1964), pp. 304-325.
10. A. A. Samarskii and E. S. Nikolaev, Methods of Solving Mesh Equations [in Russian], Moscow (1978).

EFFECT OF BRIEF THERMAL PULSES ON INTENSITY OF HEAT LIBERATION IN HELIUM BOILING

V. K. Andreev, V. I. Deev,
A. N. Savin, and K. V. Kutsenko

UDC 536.248.2:546.291

Results are offered from a study of heat liberation in boiling of liquid helium upon a heated wall under impulsive thermal action conditions.

Bubble boiling of helium is characterized by significant ambiguity in the amount of superheating of the heat liberating wall, given one and the same heat load on the heat exchange surface. Thus, it was shown in [1-4] that for slow (quasisteady-state) increase in thermal flux density the wall superheatings recorded at specified q values may be several times higher than upon subsequent reduction in thermal load. This is caused by the fact [4] that in the course of q reduction a significant fraction of the previously (upon increase in q) activated vapor formation centers continue to act, providing a high heat exchange intensity.

In [5-7] a reduction in superheating of heat liberating wall was observed in helium boiling for the case of action upon the wall by a brief light pulse. The authors of those studies assume that upon absorption of the light pulse energy the heat liberating surface emits photoelectrons, which act as vapor bubble formation centers. An increase in the number of boiling centers leads to intensification of heat exchange and reduction in wall superheating.

The present study examined the effect of short thermal pulses on heat liberation into helium boiling under large volume conditions at atmospheric pressure. The experiments were performed with the working chamber described in [8]. The heated wall consisted of a ribbon of brass foil 65 × 4 × 0.05 mm in size, thermally isolated on one side. The foil was heated by direct passage of electric current.

The operating section R_W (see Fig. 1) was connected in series with reference resistor R_r to the input of power amplifier PA. The current flowing in the circuit was set by current regulator CR. The temperature of the heat liberating surface was determined by a low-inertia germanium film resistance thermometer T. The voltage drop across the thermometer was applied to the special amplifier A, the signal from which was recorded by loop oscilloscope LO. A simultaneous recording was made of the current being fed to the working section heater. Current pulses were created by current generator G, a type G5-54. Current change over the period

Translated from Inzhenerno-Fizicheskii Zhurnal, Vol. 53, No. 3, pp. 373-376, September, 1987. Original article submitted July 4, 1986.

0022-0841/87/5303-1000$12.50